

THE OFFICIAL MAGAZINE OF THE OCEANOGRAPHY SOCIETY

Oceanography

CITATION

Dierking, W. 2013. Sea ice monitoring by synthetic aperture radar. *Oceanography* 26(2):100–111, <http://dx.doi.org/10.5670/oceanog.2013.33>.

DOI

<http://dx.doi.org/10.5670/oceanog.2013.33>

COPYRIGHT

This article has been published in *Oceanography*, Volume 26, Number 2, a quarterly journal of The Oceanography Society. Copyright 2013 by The Oceanography Society. All rights reserved.

USAGE

Permission is granted to copy this article for use in teaching and research. Republication, systematic reproduction, or collective redistribution of any portion of this article by photocopy machine, reposting, or other means is permitted only with the approval of The Oceanography Society. Send all correspondence to: info@tos.org or The Oceanography Society, PO Box 1931, Rockville, MD 20849-1931, USA.

Sea Ice Monitoring by Synthetic Aperture Radar

BY WOLFGANG DIERKING

Airborne SAR image of sea ice.
Image credit: ESA

ABSTRACT. Satellite-borne synthetic aperture radar (SAR) data are highly valuable not only for observing the open ocean but also for monitoring seasonally or permanently ice-covered ocean regions in the Arctic, Antarctic, and other areas such as the Baltic Sea, the Bohai Sea, or the Sea of Okhotsk. Fundamentals of sea ice monitoring by SAR that address the following questions are introduced: Which sea ice properties influence the radar backscattering signal directly? Which geophysical sea ice parameters are retrieved from SAR images? Important fields of recent sea ice observation activities, such as ice type classification, ice drift retrieval, and melt detection, are described. Modern satellite sensor technologies offer possibilities for significant improvements of retrieval methods, especially for more complex tasks of sea ice monitoring such as determination of ice thickness. These technologies cover enhancements of the SAR instruments themselves (multipolarization and multifrequency systems), modified mission designs (satellite constellations), and the combined use of different passive and active sensors operated in the optical, thermal, and microwave regimes.

INTRODUCTION

Since 2007, when the summer extent of Arctic sea ice reached a hitherto unexpected minimum (followed by another even lower minimum in 2012), the public has paid increased attention to recent and decadal changes of Northern Hemisphere sea ice cover. These changes are considered an indication of global warming and are expected to have a strong impact on the Arctic environment (ACIA, 2004). The information on variations in sea ice extent and concentration (the latter is the percentage of a given area of the ocean surface covered by ice) is obtained from spaceborne passive microwave radiometers that are capable of mapping the entire Arctic and Antarctic oceans within one day. Their swaths are typically about 1,500 km wide. However, they collect data only at a coarse spatial resolution of a few to tens of kilometers. Satellite scatterometers, which operate on similar spatial scales, are used to determine the areal fractions of first-year and multiyear ice (the latter has survived at least one summer season). Radar altimeters play

an important role in estimating sea ice thickness. Knowledge of the large-scale average magnitudes and variations of those ice parameters is important for climate research, for example, for validating and improving models to simulate future climate impacts on Earth's environment.

Spaceborne synthetic aperture radars (SAR) belong to a different class of sensors. Recent systems used for sea ice monitoring are operated at swath widths between 30 and 500 km and at spatial resolutions between 1 and 1,000 m. Therefore, they are well suited for observing regional and local variations of parameters characterizing the state of the sea ice cover. This means that SAR data are useful for validating results obtained from coarse-resolution radiometers and scatterometers and for developing a better understanding of local and regional interaction mechanisms between atmosphere, sea ice, and ocean, which is important for weather predictions and for climate research. SAR images are also employed by operational services charged with providing sea ice charts and forecasting ice conditions for

seasonally or perennially ice-covered waters in support of marine transportation and offshore operations.

Sea ice occurs in different stages of development. The major fraction is drifting pack ice that responds to forces exerted by wind and ocean currents. Fast ice remains in a fixed position, for example, when it is frozen to the shoreline. In the initial phase of ice growth, ice crystals appear in the uppermost water layer (frazil and grease ice). Under calm ocean conditions, smooth, elastic ice crusts up to 10 cm thick (called nilas) develop, followed by the stage of young ice (10–30 cm thick). If the ocean surface is roughened by wind, ice crystals accumulate to create pancake ice—rounded ice floes, often with rimmed edges caused by numerous collisions between single floes. Eventually, young ice or pancakes increase in thickness, and pancakes freeze together to form a closed ice cover. When the ice is 30–200 cm thick, it is called first-year ice. Multiyear ice is typically more than 2 m thick.

For sea ice observations with SAR, the main radar frequencies used cover L-band (wavelength 15–30 cm, frequency 1–2 GHz), C-band (3.8–7.5 cm, 4–8 GHz), X-band (2.4–3.8 cm, 8–12.5 GHz), and Ku-band (1.7–2.4 cm, 12.5–18 GHz). In addition to frequency, the brightness of sea ice in radar images is determined by the incidence angle and the polarization (given as a combination of transmitted and received signals, for example, “HV,” where “H” means “horizontal” and “V” is “vertical”).

Wolfgang Dierking (*wolfgang.dierking@awi.de*) is a geophysicist at the Alfred Wegener Institute for Polar and Marine Research, Bremerhaven, Germany.

Mostly, data are acquired as intensities at a preselected polarization. Modern SAR systems, such as RADARSAT-2, also provide polarimetric imaging modes—backscattered signals (intensity and phase, respectively) at HH-, VV-, HV-, and VH-polarization are measured simultaneously. For practical applications, the phase differences between signals of different polarizations are of interest. However, only the phase difference between the HH- and the VV-polarized channels reveals useful information related to the dominant scattering mechanisms from which ice properties can be inferred and ice types discriminated (Drinkwater et al., 1991). The phase differences between HH and HV or VV and VH are usually random, as there is generally little correlation between the corresponding scattering phase centers (<http://www.nrcan.gc.ca/earth-sciences/geography-boundary/remote-sensing/radar/1422>).

The objective of this article is to provide a brief general perspective of the recent status of sea ice observations using spaceborne SAR, focusing on the technological potential of modern radar and of the retrieval of different sea ice parameters from image data. First, the basic interactions between microwaves and sea ice are introduced. A detailed knowledge of these interactions is required for the interpretation of SAR imagery and for developing retrieval algorithms. The latter are used to derive geophysical parameters that characterize sea ice conditions using the measured radar intensity as input (or intensities and phases, if more radar channels are available). Then, examples of different sea ice parameters are presented with descriptions of their relevance in science

and operational mapping, and the measurement scenario at which they are optimally obtained.

SEA ICE PARAMETERS THAT INFLUENCE RADAR SCATTERING

The two major interactions between radar waves and sea ice are surface and volume scattering. At a surface that is smooth compared to the radar wavelength, the radar waves are reflected as from a mirror (specular reflection). This reflection is typical for areas where nilas and young ice are not disturbed by rafting (a process whereby pieces of thin ice slide over each other). Such areas appear very dark in SAR images. Pure resonant Bragg scattering, which is typical for the ocean surface, is less common for sea ice, because the small-scale ice roughness (on length scales of the radar waves) is spatially more irregular than ocean capillary and short gravity waves. Instead, the scattering response of a rough ice surface includes reflections of statistically distributed small planes or “facets” that are larger than the radar wavelength. In addition, researchers must account for smaller roughness elements (with sizes comparable to or less than the radar wavelength). The special characteristics of the surface structure determine the relative effects of both smaller and larger roughness elements on radar scattering. Figure 1 shows an example of an ice surface. In case of rubble (an area of compressed, broken pieces of ice) or ice ridges (broken ice accumulated into a narrow, elongated rise above the ice surface), the probability of finding surface facets directed toward the radar is much higher than for level ice. Therefore, such deformation features can be identified

as spots of bright radar returns in a SAR image. The surface roughness on first-year level ice is often on scales of the radar wavelength. Therefore, this ice type shows comparatively low radar intensities. Under calm, cold conditions, patches of saline ice crystals a few centimeters in diameter known as frost flowers grow on nilas and young ice. Frost flowers drastically increase the surface roughness. They result in strong scattering intensity at higher radar frequencies (C-, X-, and Ku-band) but are less effective scatterers at lower frequencies (L-band).

Volume scattering occurs if a fraction of the incoming radar intensity is transmitted into the ice and then redirected back to the surface by volume inclusions such as air bubbles or brine pockets (small cavities filled with high-salinity liquid that are trapped between the ice crystals). The penetration depth of a radar wave into the ice is one factor determining the efficiency of volume scattering. It decreases with increasing radar frequency, ice salinity, and temperature. Under cold conditions (temperatures at -10°C and less), the penetration depth into first-year ice with salinities between 5 and 12 (a typical range for the Arctic) is about 3–15 cm at X-band, 7–30 cm at C-band, and 0.15–1.0 m at L-band. Other factors that influence the volume scattering intensity are volume fraction, size, and shape of the inclusion particles. Large numbers of air bubbles (with sizes between tenths to a few millimeters) are found in multiyear ice but may be also present in younger ice (see Figure 1). They are of variable shape but can be well approximated as spheres when evaluating their scattering efficiency theoretically. Their volume

fraction ranges from less than 0.1 in young and first-year ice to about 0.25 in multiyear ice. The brine volume in sea ice is large during initial ice formation and growth (e.g., in nilas and young ice) and decreases at later growth stages because of desalination (i.e., the brine drains out, leaving pockets filled with

air). In particular, in the upper part of multiyear ice, the salinity is often close to zero. The radar backscattering of ice in its initial growing stage (0–10 cm thick) increases by 5–10 dB. This is explained by volume scattering from the brine pockets, which interconnect and increase in size during the process

of desalination (Nghiem et al., 1997). Brine inclusions are usually needle- or ellipsoid-shaped and are preferentially oriented along the vertical. Due to this alignment, the overall dielectric constants of, for example, nilas and young ice, are uniaxially anisotropic. Hence, these ice types reveal a non-zero phase

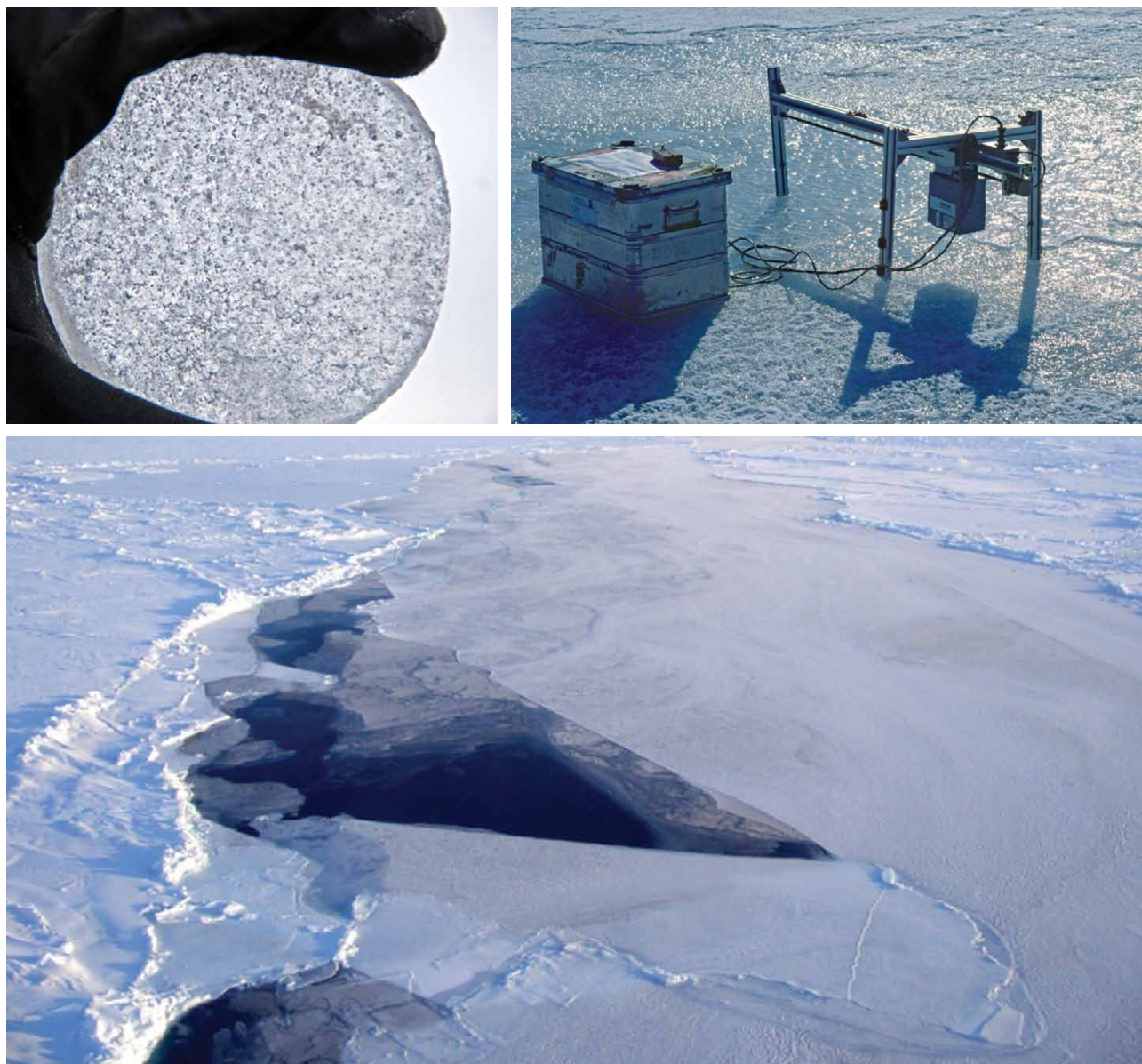


Figure 1 Different roughness scales and volume inclusions. (upper left) Air bubbles in Baltic first-year sea ice (the diameter of the ice slab is 8 cm). (upper right) Small-scale surface ripples on sea ice being measured by a laser system (photo from a field campaign in the Baltic Sea). (bottom) Deformed sea ice in Fram Strait, viewed from an airplane: includes a refrozen lead with rafted thin ice; thicker, ridged ice is visible to the left and right.

difference between the HH- and the VV-polarized signal, because the vertically and horizontally polarized radar waves travel with different wave speeds (Nghiem et al., 1995). Older ice behaves like an isotropic medium (i.e., the phase difference is zero).

“ SAR IMAGE ACQUISITIONS ARE AN IMPORTANT AND EXTREMELY VALUABLE SPACE OBSERVATION COMPONENT FOR THE RETRIEVAL OF INFORMATION ABOUT SEA ICE CONDITIONS BECAUSE THEY ARE INDEPENDENT OF LIGHT CONDITIONS AND CLOUD COVERAGE. ”

Ridges are composed of small and large ice blocks and fragments (sizes between several centimeters and a few meters) accumulated into piles by compressive forces (Figure 1). Various sizes of air voids occur between the ice fragments, and cracks occur deeper down in the ridge as well as in the ice adjacent to the ridge. These intrusions act as scattering and reflection sources, depending upon the ratio of their dimensions to radar wavelength. In freezing conditions, a layer of dry snow may develop on the ice; this changes the direction of the incoming radar beam so that its incidence angle on the ice surface becomes steeper compared to conditions without snow. The dielectric contrast between ice and snow is lower than between ice and air. Because the radar wavelength decreases in snow (the magnitude of decrease depends on the snow density), the ice surface appears rougher to the

radar. The snow grain size is between approximately 0.05 mm and 5 mm, hence, volume scattering contributions from snow can often be neglected, in particular at lower radar frequencies. Because of the relatively small dielectric contrast between snow and air and usu-

ally gentle surface undulations, surface scattering contributions from snow are also very low in most cases.

Volume scattering is reduced or completely suppressed if the snow cover and/or ice surface is wet because of melting at higher temperatures. Hence, the onset of melting on the ice can clearly be recognized if the “cold” radar signatures are dominated by the ice volume, for example, in the case of multiyear ice by scattering from air bubbles. Due to melting processes, the morphologies of the snow and ice surface change. Meltwater may penetrate to the base of the snowpack and refreeze, forming a layer of superimposed (freshwater) ice containing numerous air bubbles. Hence, when meteorological conditions change from melting to freezing or freezing to melting (during the transitions between spring and summer or summer and fall), the radar signature characteristics

of the ice may change significantly from one to the next freezing interval, giving the SAR image brightness patterns a different appearance.

The major point to keep in mind from this section is that the radar signature (signal intensity and phase) is mainly determined by small-scale ice and snow characteristics (i.e., by the characteristics of, for example, surface roughness, air bubbles, snow grains, and brine inclusions) and by ice salinity and temperature. Hence, when developing algorithms for retrieving geophysical information such as spatial distribution of ice types, duration of the melting season, or ice thickness, the major question is how these “geophysical” parameters are linked with “small-scale” sea ice properties and environmental conditions.

RETRIEVAL OF GEOPHYSICAL INFORMATION ABOUT SEA ICE CONDITIONS AND STATE

Satellite and airborne SAR systems are used for a variety of tasks regarding retrieval of information about the state of the sea ice cover (e.g., Sandven et al., 1999). Examples are monitoring of ice drift and deformation, ice type classification, observations of the marginal ice zone and of polynyas, determination of melt onset and freeze-up in the Arctic and Antarctic, quantitative characterization of ice surface topography for meteorological applications, characterization of ice growth, determination of melt pond coverage on the ice, observations of frost flower development on thin ice in conjunction with atmospheric chemistry, and gathering information about lead characteristics. In some cases, the methods developed for the retrievals can be used on an operational basis; in other

cases, they are in a premature stage. In the following, four of the applications mentioned are selected as examples and discussed in some detail. The classification of sea ice and the derivation of sea ice drift are most important for operational sea ice mapping and can be regarded as mature technologies (although there is potential for further improvements). The other examples are important applications in studies of atmosphere/sea ice/ocean interactions.

Sea Ice Drift and Deformation

Considering its independence from cloud and light conditions and its capability to “look through” dry snow, SAR is an important instrument for determining the drift and deformation patterns of sea ice. For this purpose, a sequence of SAR images acquired over the same area is needed. Forces exerted by wind and water drag and internal ice stress influence the magnitude and direction of sea ice drift. The Coriolis force and ocean surface tilt must also be taken into account. Observations of sea ice drift are of interest for a number of reasons:

- Drift systems on scales of several hundred kilometers, which are influenced by the average large-scale atmospheric circulation, affect the advective part of the sea ice mass balance in the Arctic and Antarctic. At the ice edge, ice drift patterns reflect the mesoscale ocean circulation.
- Ice drift influences the spatial and temporal distribution of heat and salinity. Heat is released at locations of ice formation and absorbed where the ice melts. Due to brine rejection during ice growth, the salinity of the water layer below the ice increases. Because old ice is of low salinity, the

upper water layer becomes less saline when the ice melts. Hence, ice growth may lead to unstable conditions in the water column below, and melting ice stabilizes the (density) stratification of the water near the surface.

- Deformation processes (ridging, rafting, formation of cracks and open leads) are related to local variations and discontinuities of ice movement. Ice drift fields derived from SAR data are, for example, used to validate model simulation of ice kinematics (Kwok et al., 2008) and to compute ice volume flux for selected areas (Kwok et al., 2010). The latter is valuable, for example, as a measure for the export of ice out of the Arctic Ocean through Fram Strait into the Greenland Sea, or through Nares Strait west of Greenland.

With SAR images, the focus is on local and regional sea ice kinematics, although a systematic data acquisition strategy, such as part of the RADARSAT Geophysical Processor System (Kwok et al., 2008), makes it possible to cover large parts of the Arctic Ocean. On scales of a few tens of kilometers up to 500 km (the latter being the typical imaging width of Wide Swath or ScanSAR mode), sea ice drift vectors can be provided at spatial resolutions of a few tens to hundred meters, mostly with good accuracy (Hollands and Dierking, 2011). With single-satellite missions, however, the achievable temporal sampling often is not sufficient. For example, when using ascending and descending orbits, the resulting time gaps are 5 and 17 hours at 78°S. This means that tidal effects or deformation processes cannot be resolved. The temporal gaps between image acquisitions can be reduced using data from satellite constellations. Drift

information can be provided as Eulerian motion on a fixed grid (Figure 2) or by continuously tracking single spots on the ice surface (Lagrangian approach).

The most popular method for retrieving ice motion from SAR images is area correlation. Using a pair or sequence of SAR images and choosing a reference area in the first image, the basic challenge is to find the respective location(s) of this area in the other image(s). A robust correlation requires a distinct and stable spatial radar intensity variation (e.g., caused by the presence of ridges and ice floe edges), which means that any deformation of the ice during movement disturbs the matching process. In principle, the window that best matches the reference area in the first image is searched in the second image within realistic ranges of displacements in all possible directions, including ice-floe rotation that may have occurred between data takes (something that happens frequently in the marginal ice zone). Because such an approach is computationally not efficient, the calculation of drift vectors is carried out using resolution pyramids and cascades (Figure 2). To construct the resolution pyramid, the original high-resolution image is gradually low-pass filtered to generate a sequence of scenes with decreasing spatial resolution. Area correlations are first calculated on the coarsest resolution level. The result is used to initialize the search on the next finer resolution level. This procedure is continued down to the original resolution. The grid on which the drift vectors are calculated remains constant in terms of length scales during the processing within one pyramid. A cascade is a sequence of coupled pyramids. The grid of drift

vectors is refined from one cascade to the next. The advantage of the cascading approach is increased robustness and a more detailed ice drift field. Rotational ice motion is not considered in the ordinary area-correlation approach and must

be treated specifically. This is a topic of recent research.

A systematic investigation of the optimal measurement scenario is yet to be done. Satellite constellations (i.e., two or more identical satellites

with coordinated ground coverage) are advantageous because the temporal gaps between single images are reduced. At lower frequencies such as L-band, deformation structures in sea ice are easier to recognize than at higher frequency,

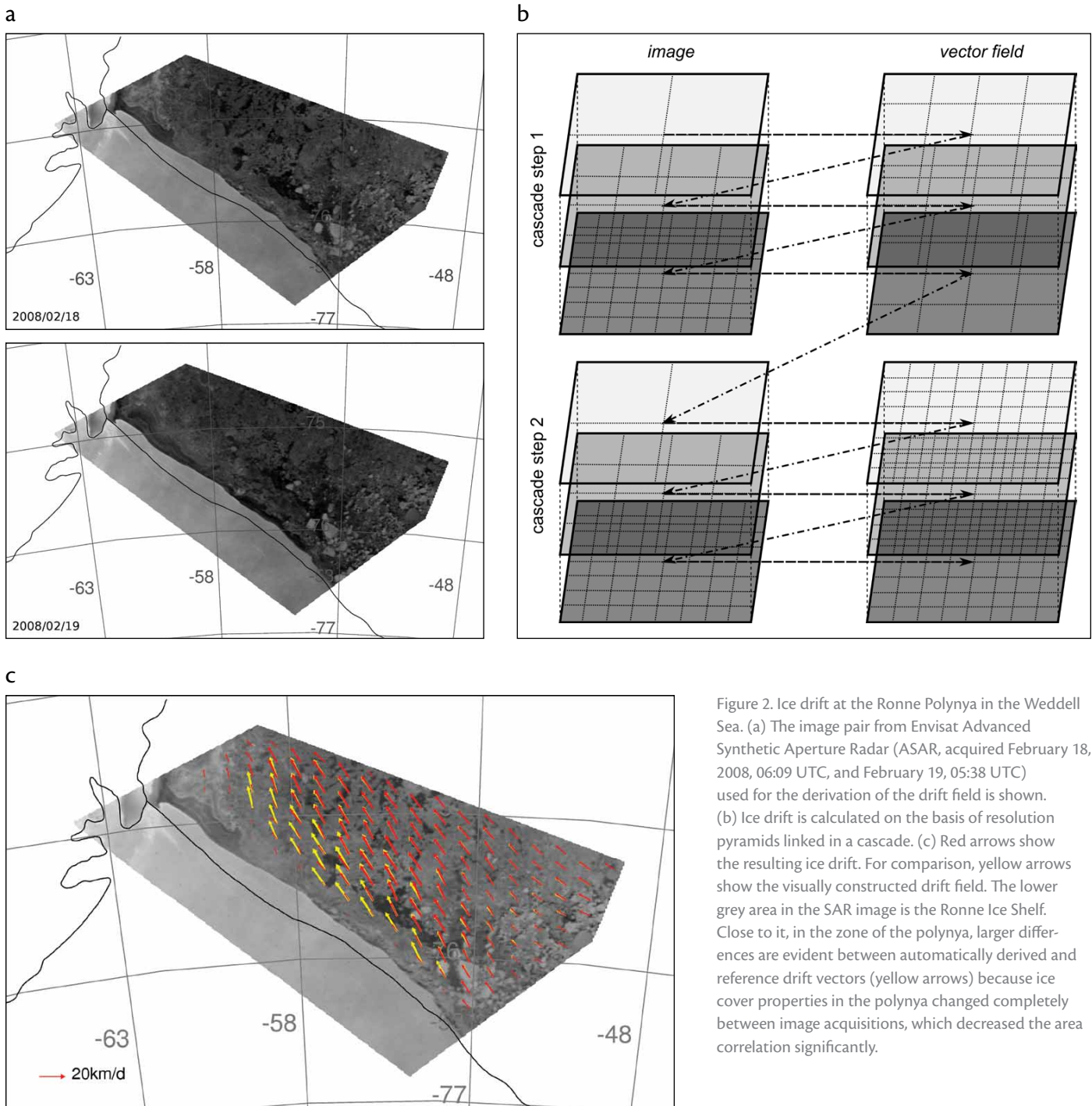


Figure 2. Ice drift at the Ronne Polynya in the Weddell Sea. (a) The image pair from Envisat Advanced Synthetic Aperture Radar (ASAR, acquired February 18, 2008, 06:09 UTC, and February 19, 05:38 UTC) used for the derivation of the drift field is shown. (b) Ice drift is calculated on the basis of resolution pyramids linked in a cascade. (c) Red arrows show the resulting ice drift. For comparison, yellow arrows show the visually constructed drift field. The lower grey area in the SAR image is the Ronne Ice Shelf. Close to it, in the zone of the polynya, larger differences are evident between automatically derived and reference drift vectors (yellow arrows) because ice cover properties in the polynya changed completely between image acquisitions, which decreased the area correlation significantly.

which improves the detection of identical intensity patterns in both images as long as ice structures do not change between the acquisitions of the first and second images. Thin ice, however, can deform easily within less than an hour, significantly changing the pattern of rafting zones. The use of low-frequency radar may be advisable during summer. Ice structures under wet snow are more difficult to recognize at melt onset and “vanish” earlier at higher than at lower frequencies. Old ice floes embedded in young ice are more difficult to recognize at L-band than at C-band or higher frequencies, which means that the latter may be a better choice for ice drift retrieval in certain ice conditions. Occasionally, it is difficult to achieve the optimal balance between the spatial resolution and the coverage (swath width), that is, to select the most appropriate SAR imaging mode.

Ice Type Classification

The goal of sea ice mapping is to retrieve different sea ice properties, to document their status at a particular time, and to follow their temporal changes. Among the most important mapping tasks is separating different ice categories or ice types from one another and from open water. This task also includes providing information about the ice deformation state, mainly about ridging and rafting. In any of these cases, it is essential that characteristic features of an ice cover can be recognized in the imagery.

Marine traffic and offshore operations in ice-covered ocean regions require maps of sea ice. They are provided by national operational ice services (Scheuchl et al., 2004). For scientific applications, the spatial distribution and

areal fraction of different ice types is useful information. As explained above, thin ice zones are areas of stronger heat exchange between the ocean and atmosphere, and brine rejection increases the release of salt into the water column below during ice formation. Zones of ice deformation reflect the impacts of wind, ocean, and internal ice stress. The decreasing ratio between the Arctic-wide multiyear and first-year ice area is an indication of large-scale changes of interaction and feedback mechanisms among the atmosphere, the ice, and the ocean.

The appearance of sea ice in radar images is affected by the frequency, polarization, incidence angle, noise level, and spatial resolution of the respective SAR system or SAR imaging mode.

- **Frequency:** Deformation structures such as ridges, rafting, rubble, and brash ice can be better discriminated from smooth level ice at L-band than at C-band and higher frequencies. C-band and higher frequencies are better suited for separating multiyear ice from the more saline first-year ice. Sea ice radar signatures at C- and X-band are usually similar, but X-band is more sensitive to properties of the surface and the subsurface layer. Because longer radar waves penetrate deeper into the ice, low-frequency SAR can, to a certain extent, be used for discriminating sea ice types during the melting period.
 - **Polarization:** HH-polarization is preferred for operational sea ice mapping. Because ocean clutter is more suppressed at HH- than at VV-polarization, the former is better suited for ice-water discrimination. At higher wind speeds, an area of open water surface appears as bright
- **Incidence angle:** The contrast between smooth level ice and rough ice increases with incidence angle. The effect is stronger at HH- than at VV-polarization. In some cases, ridges are easier to identify at larger incidence angles.
 - **Noise level:** The noise level determines the minimum detectable radar intensity. The backscattered intensity from smooth young sea ice can fall below the noise level, in particular, in the cross-polarization channels of satellite SARs. As a consequence, it is often impossible to distinguish different stages of early sea ice growth in SAR images.
 - **Spatial resolution:** In certain cases, SAR spatial resolution needs to be better than 10 m in order to achieve robust and detailed ice type classification. The separation of ice types is partly based on macroscopic ice structures with spatial scales between one and a few tens of meters (which corresponds

or even brighter than sea ice at like-polarization (HH, VV), whereas it remains relatively dark at cross-polarization (HV, VH). The separation of level and deformed ice is easier at HV- and VH-polarization because deformation zones have strong depolarization effects. Thin ice with a rough surface can be better separated from water at cross- than at like-polarization, but this is not the case for smooth thin ice. The Canadian Ice Service (CIS) has identified the following areas for which combinations of HH and HV are useful for ice analysis: detection of multiyear ice embedded in first-year ice, ice vs. open water separation, detection of leads, and ice concentration estimates.

to, for example, the width of ridges and rafting zones). Sometimes, older ice floes only a few meters in size are embedded in new ice (Figure 3). The advantage of high spatial resolution is counterbalanced by the disadvantage of a swath width limited to less than 100 km. For operational mapping, wide swath widths are preferable for obtaining frequent observations of ice-covered areas along ship routes. In such data products, the spatial resolution is on the order of 100 m so that many smaller ice structures are not recognizable (Figure 3). The consequence is a less detailed classification. A number of recent studies have addressed the use of polarimetric (“quad-pol”) data for classification. If the

sea ice cover includes fractions of thin ice, consideration of the phase difference between HH- and VV-polarization enhances classification performance (e.g., Dierking et al., 2004). When measuring in polarimetric mode, the radar signature of sea ice can be computed for any combination of transmitted and received polarization, for example, at RR- and LL-polarization (R = right circular, L = left circular). The change from one to another polarization may alter the sensitivity of the radar signal to a certain ice property (such as, for example, the degree of surface roughness or the variability of orientation angles of ice ridges; e.g., see Wakabayashi et al., 2004). Another interesting method is application of decomposition techniques

to received polarimetric radar signals. The results of decomposition can be interpreted in terms of different scattering mechanisms such as surface and volume scattering and double-bounce reflections. This information is then used to distinguish different ice types. However, in polarimetric imaging modes of recent SAR systems, the swath widths are too narrow for operational sea ice monitoring. The typical ice type classification is mainly based on ice thickness and macroscopic properties that are easy to identify visually (e.g., from the bridge of a ship). Radar, however, “sees” the sea ice differently from optical devices. Therefore, separate classification schemes need to be used for radar-based

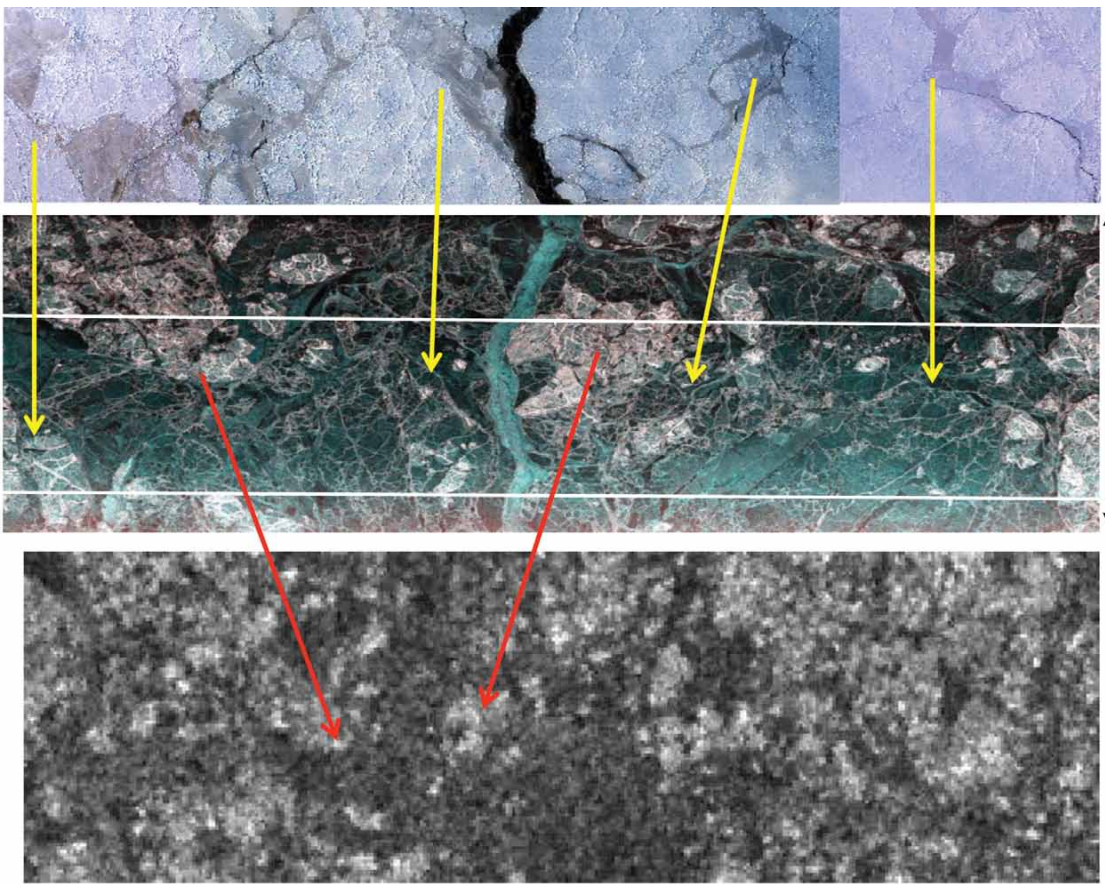


Figure 3. The pros and cons of recent SAR systems for specific sea ice mapping tasks can be assessed by comparing optical and radar images. The examples shown here were obtained on March 19, 2007, during measurements north of Svalbard. The top frame shows pictures of an airborne optical imager (spatial resolution < 1.3 m) acquired at 12:20 UTC. The middle image, acquired at 12:26 UTC, from the airborne ESAR (Enhanced SAR) system of the German Aerospace Centre, is 3 km wide with 2 m spatial resolution (Red = VH-polarization. Green = VV-polarization. Blue = VV-polarization). The bottom image is from the Envisat ASAR (wide-swath mode, spatial resolution 150 m, HH-polarization, incidence angle 26°, time 11:22 UTC).

and optical-based (field-based) data sources. It is also important to note that the appearance and discernibility of ice types in SAR images is primarily determined by ice properties, most of which are much smaller than the SAR spatial resolution (e.g., air bubbles in the ice volume and centimeter-scale surface undulations). Optimal conditions for the radar-based classification are multifrequency SAR data acquisitions (e.g., combining L-band with C- or X-band; Dierking, 2010).

An interesting option for operational sea ice services is systematic retrieval of sea ice drift and its integration into ice type classification (considering the fact that sea ice analysts usually combine data acquired on different days in order to track areas with properties confirmed by complementary data from different satellite sensors, and from aircraft and ships). Thus, zones where there are rapid changes and, in particular, deformation patterns are easier to recognize.

Melt Onset and Freeze-up

The length of the melt season strongly influences the decrease in ice mass during summer. The shift of melt onset to an earlier time is linked with corresponding temporal shifts in melt pond development, ice albedo decrease, and ocean warming. The release of freshwater from melting sea ice can alter or stop vertical circulation in the water column. Systematic observations of melt season duration and temporal shifts of melt onset and freeze-up are therefore essential for climate research (considering, for example, their influence on the decrease of summer sea ice extent). Data from passive microwave radiometers have proven useful for long-term Arctic-wide

analyses, and SAR is also a valuable data source on regional and local scales (Kwok et al., 2003). In sequences of C-band SAR images, the radar intensity of multiyear ice decreased significantly at the onset of melting conditions because the penetration depth of the radar waves is considerably reduced, eliminating backscattering from air bubbles in the ice volume. Backscattering intensity increases at freeze-up when the radar waves again penetrate deeper into the ice. The radar backscattering over first-year ice, on the other hand, may reveal an increase in intensity at melt onset (Kwok et al., 2003). Possible reasons are the growth of grains in the snow layer on the ice and/or a higher dielectric constant at the snow or ice surface due to increasing wetness. In general, higher radar frequencies are preferable for reliable detection of melt onset and freeze-up. A more robust method of detection uses not only changes in radar intensity but also magnitudes of additional parameters related to the distribution of intensity values in small image windows. In Figure 4, the onset of melt is easily recognized because backscattered radar intensity is decreased over many patches of the ice surface.

Ice Thickness

Providing information about regional and Arctic- and Antarctic-wide ice thicknesses and their spatial and temporal variations is important for estimating changes in sea ice volume, but it is one of the most challenging tasks in sea ice remote sensing. The decline of perennial ice and increased coverage of thinner seasonal ice in the Arctic, for example, changes heat transfer on scales of several hundreds of kilometers, with possible

impacts on weather and climate. In particular, the capabilities of spaceborne laser and radar altimeter systems (such as ICESat and CryoSat) for measuring ice freeboard (i.e., the part of the ice above the water level) have been extensively investigated during the last decade. In order to determine ice thickness from freeboard (under the assumption of hydrostatic equilibrium), the thickness of the snow cover as well as snow and ice density need to be known. The development of strategies for providing such data is a topic of recent investigations in sea ice remote sensing.

In this context, the use of SAR data is most promising for estimating the thickness of thinner ice on local and regional scales, in particular when using image sequences covering the time of ice formation and/or combinations of data acquired at different polarizations. A number of investigators noted correlations between ice thickness and different radar parameters such as intensity (at different polarizations) and the co-polarization ratio HH/VV (e.g., Wakabayashi et al., 2004; Nakamura et al., 2009). The observed increase in the backscattering coefficient during early sea ice growth and changes in sea ice properties linked with growing thickness (e.g., vertical dielectric profile and size of brine inclusions) may explain such correlations. The difference between radar intensities at VV- and HH-polarization is relatively sensitive to the dielectric constant of the near-surface ice layer, which is, in turn, related to ice thickness via corresponding changes in near-surface ice salinity. In one study from the Antarctic, even ice thicknesses up to about 1.2 m could be retrieved with reasonable accuracy based

on the co-polarization ratio at C-band (Nakamura et al., 2009). Correlations between ice thickness and radar signature are similar at L- and C-band. Because the L-band radar signature is often less affected by the small-scale roughness of the ice surface but is more strongly influenced by deeper portions of the ice, its use may offer an advantage. On the other hand, the scattering intensity from thin ice is lower and hence closer to (or even below) the noise level at L-band. In one direct comparison,

L-band radar was less sensitive to ice thickness compared to C-band (Kwok et al., 1995). It has also to be emphasized that “disturbing” factors such as frost flowers or rafting processes that influence the radar signature have to be taken into account and may overlay the effect of ice growth. Correlations were also found for thicker ice classes, even when using only radar intensity. In this special case, it was speculated that surface roughness, at both small and large scales, was changing with ice age.

CONCLUSION

SAR image acquisitions are an important and extremely valuable space observation component for the retrieval of information about sea ice conditions because they are independent of light conditions and cloud coverage. With recent satellite SAR instruments, multi-polarization and multifrequency data have proven to be essential for retrieval of various sea ice parameters such as ice type distribution and drift. SAR images are employed for operational mapping of

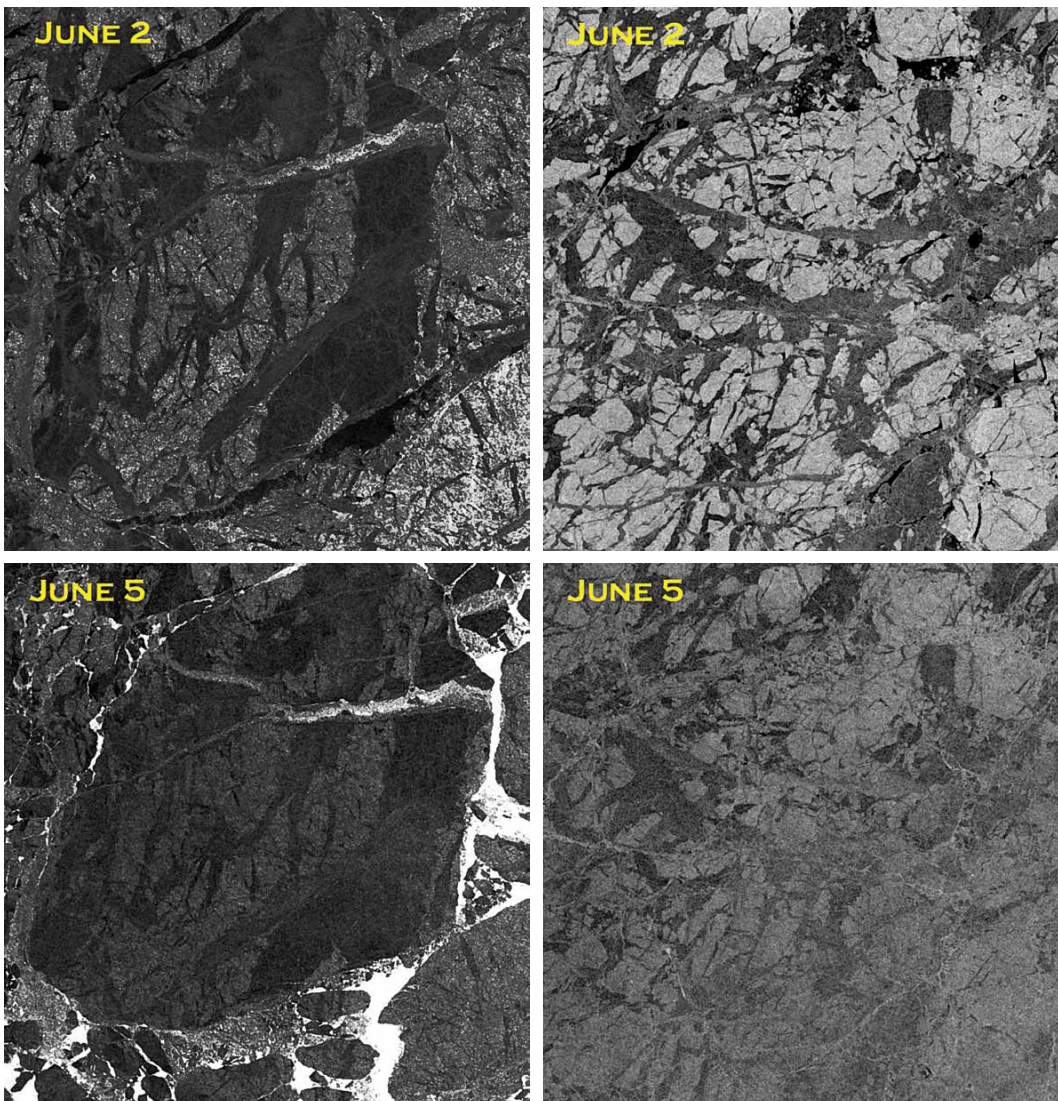



Figure 4. Example from the Beaufort Sea, showing how melting conditions change the appearance of sea ice in Envisat ASAR images (acquired in wide-swath mode at HH-polarization). The images in the upper row were acquired on June 2 at 20:27:40 UTC, and those at the bottom on June 5 at 20:33:24 UTC. The incidence angles are between 19° and 28° for the images on the left side and between 35° and 43° on the right side. The images cover an area of approximately 90 km × 90 km. On June 2, temperatures were below the freezing point; on June 5, melting had begun, which caused a decrease in radar intensities and intensity contrasts between different zones of the ice cover. Note that the ice drifted during the three days between data acquisitions.

sea ice conditions to serve marine traffic and offshore operations. In science applications, they play an important role in permitting observations of local and regional processes such as ice deformation or ice growth and melt. SAR observations are also useful for validating results of computer models that simulate the kinematics and dynamics of sea ice in the Arctic and Antarctic at spatial resolutions of about 10 km and less. SAR images are valuable for assessing the quality of data products obtained from spaceborne coarse-resolution instruments such as microwave radiometers and scatterometers.

In particular, images acquired at different frequencies provide complementary information. Because sea ice is a very dynamic medium whose spatial patterns and structures can change within hours, SAR constellation missions such as Sentinel-1 or RCM (RADARSAT Constellation Mission) increase the potential for providing the spatial and temporal sampling crucial for sea ice monitoring. Several studies indicate, however, that the retrieval of parameters characterizing a number of important sea ice processes (such as the evolution of polynyas) requires the simultaneous use of different sensor types (passive and active, operating in the optical, thermal, and microwave parts of the electromagnetic spectrum). For the development of reliable and robust retrieval algorithms that are necessary for relating satellite measurements to sea ice conditions, the acquisition of corresponding field data in the vast polar regions remains a challenge that requires enhanced international efforts. Closer and more intense collaboration between operational sea ice service centers and

research institutes dealing with sea ice research is mandatory for advancing sea ice monitoring and modeling/forecasting sea ice conditions.

ACKNOWLEDGEMENTS

I would like to thank my colleagues Stefanie Linow and Thomas Hollands for providing parts of the figures. I express my gratitude to Matt Arkett and two anonymous reviewers. Because of their constructive comments, nonspecialists will find the text easier to read. This work was supported by the project “SIDARUS” (Sea Ice Downstream services for Arctic and Antarctic Users and Stakeholders) in the Seventh Framework Programme of the European Community for Research, Technological Development and Demonstration Activities under the funding scheme of “Collaborative Project,” Grant 262922. 

REFERENCES

- ACIA (Arctic Climate Impact Assessment). 2004. *Impacts of a Warming Arctic*. Cambridge University Press, 140 pp. Available online at <http://www.acia.uaf.edu> (accessed June 19, 2013).
- Dierking, W. 2010. Mapping of different sea ice regimes using images from Sentinel-1 and ALOS synthetic aperture radar. *IEEE Transactions on Geoscience and Remote Sensing* 48(3):1,045–1,058, <http://dx.doi.org/10.1109/TGRS.2009.2031806>.
- Dierking, W., H. Skriver, and P. Gudmandsen. 2004. On the improvement of sea ice classification by means of radar polarimetry. Pp. 203–209 in *Remote Sensing in Transition: Proceedings of the 23rd Symposium of the European Association of Remote Sensing Laboratories*, Ghent, Belgium, June 2–5, 2003. Rudi Goossens, ed., Millpress, Rotterdam.
- Drinkwater, M.R., R. Kwok, D.P. Winebrenner, and E. Rignot. 1991. Multifrequency polarimetric synthetic aperture radar observations of sea ice. *Journal of Geophysical Research* 96(C11):20,679–20,698, <http://dx.doi.org/10.1029/91JC01915>.
- Hollands, T., and W. Dierking. 2011. Performance of a multi-scale correlation algorithm for the estimation of sea ice drift from

- SAR images: Initial results. *Annals of Glaciology* 52(57):311–317, <http://dx.doi.org/10.3189/172756411795931462>.
- Kwok, R., C.F. Cunningham, and S.V. Nghiem. 2003. A study of the onset of melt over the Arctic Ocean in RADARSAT synthetic aperture radar data. *Journal of Geophysical Research* 108, 3363, <http://dx.doi.org/10.1029/2002JC001363>.
- Kwok, R., E.C. Hunke, W. Maslowski, D. Menemenlis, and J. Zhang. 2008. Variability of sea ice simulations assessed with RGPS kinematics. *Journal of Geophysical Research* 113, C11012, <http://dx.doi.org/10.1029/2008JC004783>.
- Kwok, R., S.V. Nghiem, S.H. Yueh, and D.D. Huynh. 1995. Retrieval of thin ice thickness from multifrequency polarimetric SAR data. *Remote Sensing of Environment* 51:361–374, [http://dx.doi.org/10.1016/0034-4257\(94\)00017-H](http://dx.doi.org/10.1016/0034-4257(94)00017-H).
- Kwok, R., L. Toudal Pedersen, P. Gudmandsen, and S.S. Pang. 2010. Large sea ice outflow into the Nares Strait in 2007. *Geophysical Research Letters* 37, L03502, <http://dx.doi.org/10.1029/2009GL041872>.
- Nakamura, K., H. Wakabayashi, S. Uto, S. Ushio, and F. Nishio. 2009. Observation of sea-ice thickness using ENVISAT data from Lützow-Holm Bay, East Antarctica. *IEEE Geoscience and Remote Sensing Letters* 6(2):277–281, <http://dx.doi.org/10.1109/LGRS.2008.2011061>.
- Nghiem, S.V., R. Kwok, S.H. Yueh, and M.R. Drinkwater. 1995. Polarimetric signatures of sea ice. Part 1. Theoretical model. *Journal of Geophysical Research* 100(C7):13,665–13,679, <http://dx.doi.org/10.1029/95JC00937>.
- Nghiem, S.V., R. Kwok, S.H. Yueh, A.J. Gow, D.K. Perovich, J.A. Kong, and C.C. Hsu. 1997. Evolution in polarimetric signatures of thin saline ice under constant growth. *Radio Science* 32(1):127–151, <http://dx.doi.org/10.1029/96RS03051>.
- Sandven, S., O.M. Johannessen, M.W. Miles, L.H. Pettersson, and K. Kloster. 1999. Barents Sea seasonal ice zone features and processes from ERS 1 synthetic aperture radar: Seasonal Ice Zone Experiment 1992. *Journal of Geophysical Research* 104(C7):15,843–15,857, <http://dx.doi.org/10.1029/1998JC900050>.
- Scheuchl, B., D. Flett, R. Caves, and I. Cumming. 2004. Potential of RADARSAT-2 data for operational sea ice monitoring. *Canadian Journal of Remote Sensing* 30(3):448–461, <http://dx.doi.org/10.5589/m04-011>.
- Wakabayashi, H., T. Matsuoka, K. Nakamura, and F. Nishio. 2004. Polarimetric characteristics of sea ice in the Sea of Okhotsk observed by airborne L-band SAR. *IEEE Transactions on Geoscience and Remote Sensing* 42(11):2,412–2,425, <http://dx.doi.org/10.1109/TGRS.2004.836259>.